frontiers in Marine Science

BRIEF RESEARCH REPORT
published: 08 September 2020
doi: 10.3389/fmars.2020.00713

Dissolved and Particulate Primary Production and Subsequent Bacterial C Consumption in the Southern East China Sea

Tzong-Yueh Chen[1,2], Chao-Chen Lai[3], Fuh-Kwo Shiah[1,3,4] and Gwo-Ching Gong[1,2]**

[1] Institute of Marine Environment and Ecology, National Taiwan Ocean University, Keelung, Taiwan, [2] Center of Excellence for the Oceans, National Taiwan Ocean University, Keelung, Taiwan, [3] Research Center for Environmental Changes, Academia Sinica, Taipei, Taiwan, [4] Institute of Oceanography, National Taiwan University, Taipei, Taiwan

Dissolved primary production (DPP), particulate primary production (PPP), and the subsequent bacterial production (BP) and respiration (BR) were reported for the first time in the NW Pacific. The study area of the subtropical southern East China Sea covers different water types, including oligotrophic Kuroshio and Taiwan Strait waters, as well as nutrient-rich China coastal and upwelled Kuroshio subsurface waters. On an areal basis, DPP and PPP ranged from 67–1649 and 160–1182 mgC m^{-2} d^{-1}, respectively, showing high values in the upwelling area. The contribution of DPP to total primary production (percent extracellular release; PER) averaged 40.8 ± 12.2% with >50% in the upwelling stations. The BP and BR ranged from 48–245 and 709–2822 mgC m^{-2} d^{-1}, respectively, showing patterns similar to those of primary production. Bacterial growth efficiency (BGE) averaged 5.7 ± 1.4%, representing the lower end of global ocean values. Phytoplankton and bacteria were well coupled in the upwelling area, whereas primary production could not sustain the bacterial carbon demand (BCD) at other stations. The slope of the log–log relationship between DPP and PPP was >1, indicating that the microbial loop may receive relatively less organic carbon supply in the future warmer, less productive ocean.

Keywords: dissolved primary production, particulate primary production, percent extracellular release, bacterial production, bacterial respiration

OPEN ACCESS

Edited by:
Carol Robinson, University of East Anglia, United Kingdom

Reviewed by:
Alex J. Poulton, The Lyell Centre, United Kingdom
X. Antón Álvarez-Salgado, Consejo Superior de Investigaciones Científicas (CSIC), Spain

****Correspondence:***
Tzong-Yueh Chen
tzongyueh.chen@gmail.com
Gwo-Ching Gong
gcgong@mail.ntou.edu.tw

Specialty section:
This article was submitted to Marine Biogeochemistry, a section of the journal Frontiers in Marine Science

Received: *09 March 2020*
Accepted: *05 August 2020*
Published: *08 September 2020*

Citation:
Chen T-Y, Lai C-C, Shiah F-K and Gong G-C (2020) Dissolved and Particulate Primary Production and Subsequent Bacterial C Consumption in the Southern East China Sea. Front. Mar. Sci. 7:713. doi: 10.3389/fmars.2020.00713

INTRODUCTION

Photosynthesis is the most important organic carbon source in the ocean (Druffel et al., 1992). Particulate primary production [particulate primary production (PPP); i.e., the carbon fixed in the particulate form] could be transported to higher trophic levels through grazing food webs, whereas dissolved primary production (dissolved primary production (DPP); i.e., photosynthetic carbon released by phytoplankton) fuels the microbial loop. DPP has long been recognized as a source of labile organic carbon for heterotrophic bacterial growth (e.g., Cole et al., 1982; Norrman et al., 1995). However, DPP is often omitted or only roughly estimated in budgets of the marine organic carbon cycle (Thornton, 2014). In fact, DPP varies from <0.01 to >100 mgC m^{-3} h^{-1} in natural marine waters, which leads to its percent extracellular release [PER; = DPP/(DPP + PPP)] ranging

from <1 to ∼100% in the world's ocean (Baines and Pace, 1991; Nagata, 2000; Agustí and Duarte, 2013; Wyatt et al., 2014). It is therefore necessary to understand DPP variations to obtain a better estimate of global carbon fluxes.

The East China Sea (ECS), located in the subtropical northwestern Pacific, is one of the largest marginal seas in the world.Four water masses affect the hydrography in the southern ECS (Gong et al., 1996): nutrient-rich China coastal waters, oligotrophic Taiwan Strait waters, oligotrophic Kuroshio waters, and topographically upwelled Kuroshio subsurface waters. In this area, inorganic nutrients could be brought to the system from riverine input from the coast of China (i.e., station 1 in **Figure 1**) or from the Kuroshio upwelling that occurs at the shelf break northeast of Taiwan (i.e., stations 9 and 11 in **Figure 1**). Large variability of biological activities (PPP and bacterial production were 90–2133 and 28–329 mgC m^{-2} d^{-1}, respectively) (Shiah et al., 2000) has been reported in this area, showing that high biological productivities occurred with high nutrient inputs. The complicated hydrography caused by the interactions between different water masses in this area could also lead to dynamic microbial carbon fluxes.

The DPP contribution to total primary production (TPP; = PPP + DPP) usually ranges between 10 and 30% (Baines and Pace, 1991; Nagata, 2000). Given that the DPP is generally composed of labile organic matter, autochthonous DPP is considered to sustain heterotrophic bacterial growth in the ocean (Norrman et al., 1995; Amon et al., 2001). Heterotrophic bacteria can either take up or respire photosynthetically fixed DPP for their growth or maintenance of metabolic needs. The amount of photosynthetically fixed carbon that can flow through the microbial loop is controlled by the bacterial growth efficiency [BGE; = bacterial production (BP)/bacterial carbon demand (BCD); BCD = BP + bacterial respiration (BR)]. However, the BGE varies in a large range of <5–60% in marine systems (del Giorgio and Cole, 1998; Robinson, 2008). Although little is known about what controls the wide range of BGE values, the relationship between BGE and BP has been systematically determined. Due to the difficulties in directly measuring BR, BGE is often derived from these published BGE:BP (e.g., del Giorgio and Cole, 1998; Robinson, 2008) rather than direct measurements.

As photosynthesis is the ultimate organic carbon source in the open ocean, bacterial and primary production are generally positively correlated (Cole et al., 1988). BP averaged 20% (volumetric) or 30% (areal) of PPP in a cross-system review (Cole et al., 1988). The strength of the "coupling" between phytoplankton and bacteria is considered to represent the importance of phytoplankton and can be used to determine how phytoplankton-produced material supports bacterial growth. Phytoplankton and bacteria are strongly coupled in the open ocean (e.g., Morán et al., 2002). However, weak coupling has also been reported (e.g., Duarte et al., 2005). Recently, there have been some debates about phytoplankton-bacteria coupling and decoupling (Fouilland and Mostajir, 2010; Morán and Alonso-Sáez, 2011; Huang et al., 2019a). In the open ocean where dissolved organic carbon (DOC) is mainly autochthonous, phytoplankton and bacteria are usually coupled (Morán et al., 2002). On the other hand, Fouilland and Mostajir (2010) suggested that BCD always exceeds phytoplankton primary production.

Most DPP studies have been conducted in the temperate North Atlantic Ocean, the Mediterranean Sea, and polar regions (e.g., Morán et al., 2002; Marañón et al., 2004; López-Sandoval et al., 2011). There has been only one DPP study in the NE Pacific (Anderson and Zeutschel, 1970), while no study has been performed in the NW Pacific. Here, we report direct measurements of complete microbial fluxes of photosynthesized carbon, including DPP, PPP, BP, and BR, in the subtropical southern ECS of the NW Pacific for the first time. Our main objectives were (1) to quantify the DPP and its contribution to the TPP (i.e., PER); (2) to quantify BP, BR, and BGE; and (3) to assess the extent to which DPP can sustain the BCD.

MATERIALS AND METHODS

Study Area and Sampling

The cruise was carried out in the subtropical southern ECS (**Figure 1**) on R/V Ocean Researcher II during 16–21 May 2018. The sampling transect extends from the shelf near the coast of China to the shelf slope region where the Kuroshio Current induces topographic upwelling (Gong et al., 1996). Seawater samples (one sample from each depth unless indicated) were collected from four to six depths at each station (see **Figure 2** for exact sampling depths) using a rosette sampler with 20-L Teflon-coated X-Niskin bottles (General Oceanics, United States) and a mounted CTD (Seabird, United States). Photosynthetically active radiation (PAR) above the sea surface was measured during the cruise using an irradiance meter (Biospherical, United States). In addition to temperature and salinity, depth profiles of underwater PAR (Chelsea Technologies, United Kingdom) were also recorded. The light attenuation coefficient (K_d) was then calculated from the depth profile of PAR. The euphotic zone depth (Z_e) was defined as the depth where 1% surface PAR remains and could be estimated as $4.605/K_d$.

Chemical Determinations

Particulate material was defined as the material retained on a pre-combusted GF/F filter (Whatman; i.e., particles larger than the nominal pore size of 0.7 μm), while dissolved material was defined as the material which passed through the GF/F filter. The DOC concentrations were determined by the high-temperature catalytic oxidation (HTCO) method on a Shimadzu TOC-V analyzer (Wurl, 2009). Nutrient (nitrate, nitrite, phosphate, and silicate) samples were collected in acid-washed polypropylene bottles, immediately frozen in liquid nitrogen, and kept at −20°C until analysis. Nitrate was reduced to nitrite using cadmium-copper filings, and concentrations were determined by the diazo-pink method (Parsons et al., 1984). Nitrite concentrations were determined the same way as nitrate but excluding the reduction process. Phosphate concentrations were determined by the molybdenum-blue method (Parsons et al., 1984), and silicate concentrations were determined by the molybdate-blue method (Parsons et al., 1984). Samples for chlorophyll *a* (Chl)

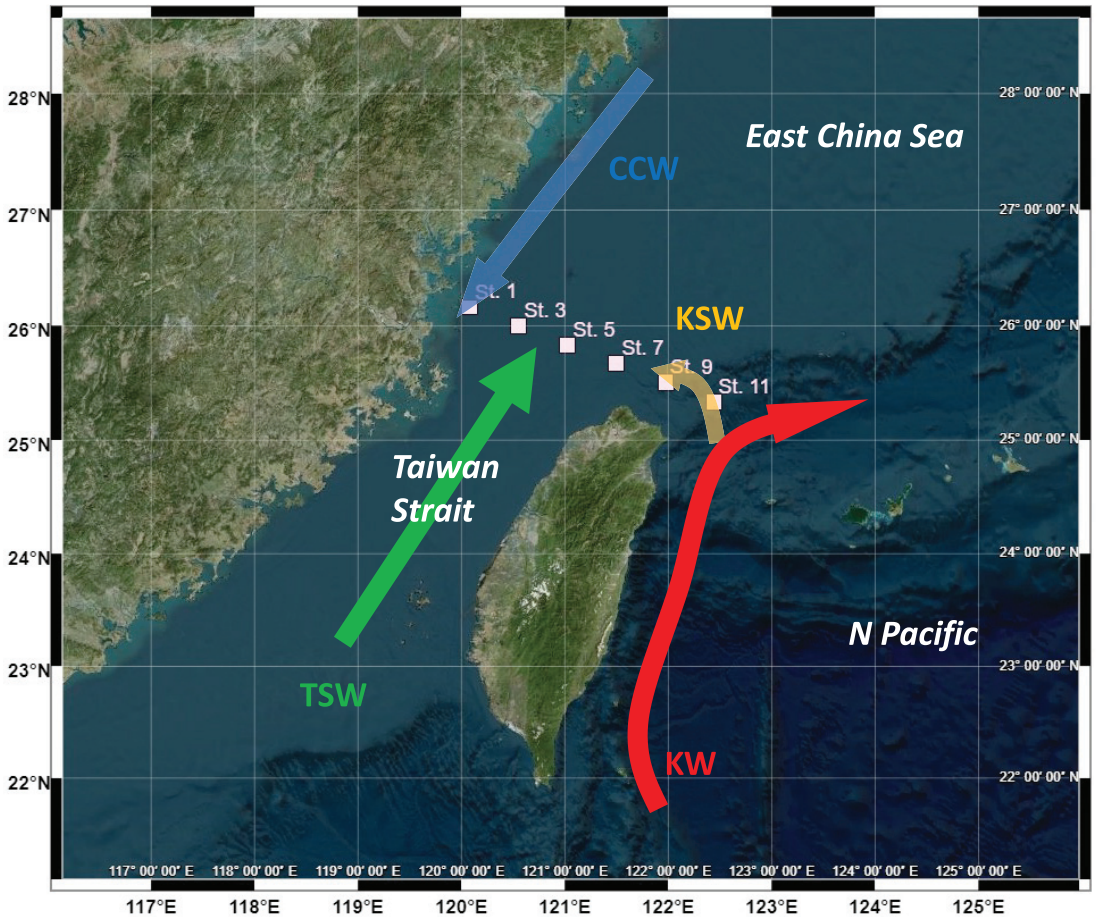

FIGURE 1 | Sampling sites with different water masses. KW denotes Kuroshio waters; KSW denotes upwelling Kuroshio subsurface waters; TSW denotes Taiwan Strait waters; CCW denotes China coastal waters.

were collected on GF/F filters and kept at−20°C until analysis. Chl was extracted with 90% acetone, and concentrations were determined using a fluorometer (Parsons et al., 1984).

Photosynthesis-Irradiance (P^B–E) Experiments

Primary production was determined by the ^{14}C assimilation method (Parsons et al., 1984). In brief, seawater samples of P^B–E were collected at two depths at each station within the euphotic layer (surface and subsurface of 20 or 25 m). P^B–E curves were obtained in a surface seawater-cooled incubator with artificial illumination (100 Watt). Samples with 10 μ Ci of ^{14}C addition were incubated at nine different PAR levels (2000, 1365, 950, 800, 480, 400, 260, 130, 0 μ Einstein m^{-2} s^{-1}; 1 Einstein (E) = 1 mole photon; one bottle for each PAR level). After 2 h of incubation, PPP subsamples were collected on GF/F filters, while DPP subsamples of 5 mL were collected as the filtrate passing through a 0.22-μm filter (Millipore). Note that PPP could potentially be overestimated due to DOC retention by the filters (e.g., Abdel-Moati, 1990; Moran et al., 1999; Novak et al., 2019). After HCl acidification and addition of the scintillation cocktail, DPP and PPP were measured as the radioactivity on a liquid scintillation counter (Tri-Carb 2800TR, PerkinElmer). The depth profiles of PPP and DPP were modeled using the P^B–E relationship according to Webb et al. (1974) or Platt et al. (1980). The daily depth-integrated primary production was then be calculated using the trapezoid method (see more detail in **Appendix 1**).

Heterotrophic Bacteria

Bacterial abundance and production were determined at all sample depths by flow cytometric counting (Gasol and del Giorgio, 2000) and ^3H-thymidine incorporation (Fuhrman and Azam, 1982), respectively. For bacterial abundance analysis, water samples were collected in 2 mL polypropylene tubes, preserved with paraformaldehyde (PFA; 1% final concentration), placed in liquid nitrogen, and kept at −80°C until analysis. Samples were then stained with SYBR Green I and counted on a flow cytometer (CyFlow, PARTEC) with internal bead standards. For BP analysis, triplicate water samples with ^3H-thymidine addition were incubated at *in situ* temperature for 2 h. Incubation was terminated by formaldehyde, and samples were kept in

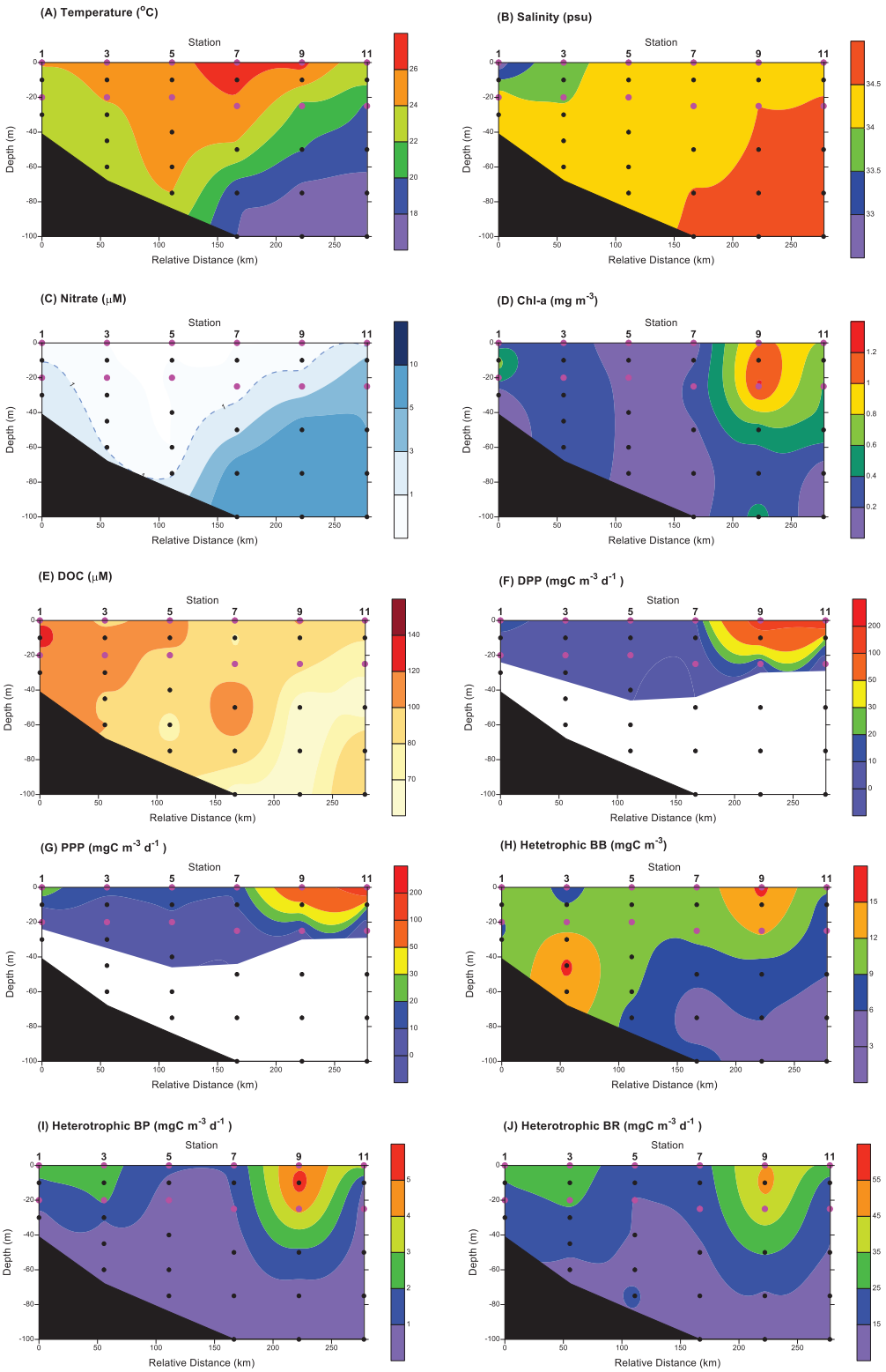

FIGURE 2 | Vertical distribution of **(A)** temperature; **(B)** salinity; **(C)** nitrate; **(D)** chlorophyll *a*; **(E)** dissolved organic carbon (DOC); **(F)** dissolved primary production (DPP); **(G)** particulate primary production (PPP); **(H)** heterotrophic bacterial biomass(BB); **(I)** heterotrophic bacterial production (BP); **(J)** heterotrophic bacterial respiration (BR). DPP and PPP values were modeled from P^B–E curves and BR values were derived from BP at the same depth as BR = $6.21*BP^{0.56\pm0.13}$ (r^2 = 0.66; $p < 0.01$; n = 12). Black dots denoted sampling depths; and pink dots denoted where the photosynthesis-irradiance experiments and BR were performed.

the refrigerator until analysis. The thymidine incorporation rate was measured as the radioactivity on a liquid scintillation counter (Tri-Carb 2800TR, PerkinElmer). Bacterial biomass and production in C units were estimated using thymidine and carbon conversion factors of 1.18×10^{18} cell mole^{-1} (Fuhrman and Azam, 1982) and 2×10^{-14} gC cell^{-1} (Ducklow, 2000), respectively. Direct measurements of BR were performed at the same two depths from each station as sampled P^B–E described above. A total of 12 BR samples were prefiltered through a 1.2-μm-pore-size membrane, and the initial dissolved oxygen (DO) concentrations with triplicates were recorded. Triplicate subsamples from each depth were then incubated in 300 mL BOD bottles for 48 h in the dark, while cooled with running surface seawater, and final DO concentrations were immediately determined using a modified Winkler method (Pai et al., 1993). The Redfield ratio of 106:138 (C:O_2) was used as the respiratory quotient (RQ).Note that incubations of pre-filtered water samples for longer than 24 h may lead to an overestimation of BR (see more detail in **Appendix 2**).

Data Analysis

JMP software (SAS Institute, United States) was used for statistical analysis. Unless otherwise indicated, variation around each mean is presented as ± one standard deviation. All depth-integrations were calculated down to 100 m or the bottom depth of the seabed if that was shallower except PPP and DPP. PPP and DPP were integrated down to the bottom of the euphotic zone.

RESULTS

Hydrological and Biogeochemical Data

The surface temperature ranged from 23.07–26.80°C with a mean value of 25.10 ± 1.43°C. Low temperatures occurred at station 1 (24.08°C) and station 11 (23.07°C), indicating the effect of riverine input and topographic upwelling, respectively (**Figure 2A**). The surface salinity ranged from 32.66–34.39 with a mean value of 33.93 ± 0.65, showing a minor freshwater effect at nearshore station 1 (**Figure 2B**). The vertical distribution of seawater temperature (**Figure 2A**) further verified the upwelling occurring at stations 9 and 11. The nitrate concentration ranged from <0.01–9.12 μM with an average of 2.39 ± 3.06 μM (**Figure 2C**); the phosphate concentration ranged from <0.03–0.83 μM with an average of 0.28 ± 0.23 μM; the silicate concentration varied from 1.4–16 μM with an average of 6.6 ± 3.9 μM. The vertical distribution of nutrients was similar, as strong upwelling occurred in the eastern transect (as the example of nitrate in **Figure 2C**). The Chl concentration ranged from 0.02–1.24 mg m^{-3} with an average of 0.36 ± 0.31 mg m^{-3} (**Figure 2D**). The spatial distribution of Chl did not resemble the patterns of the hydrography or nutrients. The highest Chl concentration occurred at upwelling station 9, whereas Chl at the strongest upwelling station 11 was only slightly higher than the average. The DOC concentration ranged from 64–149 μM with a mean value of 92 ± 19 μM (**Figure 2E**). The spatial distribution of DOC showed that high concentrations occurred nearshore and decreased offshore, indicating potential riverine or terrestrial sources.

Primary Production

Based on the P^B–E relationship, PPP ranged from 0.5–176 mgC m^{-3} d^{-1}, while DPP ranged from 0.3–166 mgC m^{-3} d^{-1} (**Figures 2F,G**). Both PPP and DPP appeared to have extremely high values at upwelling stations 9 and 11 and generally decreased with depth. PER ranged from 24.9–62.0%, and showed high values (>50%) at upwelling stations 9 and 11.

Heterotrophic Bacterial Parameters

Bacterial biomass (BB) ranged from 3.5–15.7 mgC m^{-3} with high values in the surface water and lower values at depth (**Figure 2I**). BP varied from 0.32–5.49 mgC m^{-3} d^{-1} and exhibited a similar vertical distribution as bacterial biomass (**Figure 2J**). Direct measurements of BR ranged from 11–53 mgC m^{-3} d^{-1}(CV < 10%). BR could be derived from this relationship for those depths where BP was measured (see Discussion and **Appendix 3**).

$$\mathrm{BR_{est}} = 6.21 * \mathrm{BP}^{0.56\pm0.13} (r^2 = 0.66; p < 0.01; n = 12)$$

The derived BR values (BR_{est}) ranged from 9.8–48 mgC m^{-3} d^{-1} with a mean value of 21 ± 10 mgC m^{-3} d^{-1}. BCD could then be calculated as BCD = BP + BR_{est}. The calculated BCD ranged from 10–54 mgC m^{-3} d^{-1} with an average of 22 ± 11 mgC m^{-3} d^{-1}.

DISCUSSION

Depth-Integrated Microbial Carbon Fluxes

The partitioning of photosynthetically fixed carbon into dissolved and particulate phases directly controls the microbial organic carbon fluxes. Therefore, the PER is important to assess the quantitative role of DPP. In this study, we calculated the areal PPP, DPP, and PER from P^B–E relationships. The depth-integrated PPP (IPPP) ranged from 160–1182 mgC m^{-2} d^{-1} with a mean value of 540 ± 467 mgC m^{-2} d^{-1}, while the depth-integrated DPP (IDPP) ranged from 67–1649 mgC m^{-2} d^{-1} with a mean value of 555 ± 683 mgC m^{-2} d^{-1} (**Table 1**). The IPPP and IDPP resulted in daily PER values ranging from 28.6–60.1% with a mean value of 40.8 ± 12.2%. The IPPP values were comparable to those measured in a previous study of 695 ± 562 mgC m^{-2} d^{-1} (Shiah et al., 2000), showing that high IPPP occurred in the upwelling stations. IDPP showed a similar spatial pattern as IPPP: extremely high productivity in the upwelling area. The daily PER in this study was higher than the average PER of 13% across diverse aquatic ecosystems (Baines and Pace, 1991) and the general range of 10–20% in the world's oceans (Nagata, 2000). PER has been found to be related to environmental variables (such as irradiance and nutrient concentrations) and cell physiology (growth or stationary phase). High PER has been observed near the surface with high irradiance (Thomas, 1970; Berman and Holm-Hansen, 1974). However, a negative correlation between PER and irradiance has also been reported

TABLE 1 | Depth-integrated microbial fluxes of photosynthesized carbon.

Station	Z_e (m)	Z_m (m)	PPP (mgC m^{-2} d^{-1})	DPP (mgC m^{-2} d^{-1})	PER (%)	BP (mgC m^{-2} d^{-1})	BR (mgC m^{-2} d^{-1})	BGE (%)	TPP:BCD (%)
1	24	11	272	156	36.5	48	709	6.4	56.5
3	35	21	160	67	29.6	77	1147	6.3	18.6
5	46	23	277	111	28.6	57	1218	4.5	30.5
7	44	14	252	167	39.9	67	1445	4.4	27.7
9	30	8	1095	1649	60.1	245	2822	8.0	89.5
11	29	6	1182	1181	50.0	72	1459	4.7	154.3

Z_e and Z_m denoted the depths of the euphotic zone and mixed layer, respectively. PPP and DPP denote particulate and dissolved primary production, respectively; TPP denotes total primary production (=PPP+DPP); PER denotes percent extracellular release; BP and BR denote heterotrophic bacterial production and respiration, respectively; BCD denotes bacterial carbon demand (=BP+BR); BGE denotes bacterial growth efficiency (=BP/BCD).

(e.g., Morán and Estrada, 2001; Marañón et al., 2004). We found that the PER and irradiance were not significantly correlated in this study. Nutrient conditions have also been reported to affect PER. Varela et al. (2006) found that PER was the highest when phytoplankton used nitrate as the nitrogen source, whereas PER was lower during the uptake of ammonium and urea. The influence on PER of the composition of inorganic nitrogen may partially explain the PER distribution in the southern ECS. At upwelling stations (9 and 11), high levels of nitrate input from the deep ocean could lead to high PER values. In oligotrophic stations 3 and 5, where regenerated ammonium was likely the dominant source for phytoplankton uptake (Dugdale and Goering, 1967), the system would have lower PER. Stations 1 and 7 may receive additional nitrate from terrestrial sources and weak upwelling; thus, PER values were between upwelling and oligotrophic stations. Huang et al. (2019b) also indicated that mixing of different water masses could affect biological activities.

The BCD, which is composed of bacterial production and respiration, is responsible for the major consumption of photosynthetically fixed carbon. The depth-integrated BP (IBP) ranged from 48–245 mgC m^{-2} d^{-1}, showing the highest BP at upwelling station 9 (**Table 1**). The IBP accounted for an average of 23.6 ± 13.9% of IPPP, which was comparable to the global average of 30% (Cole et al., 1988). Unlike BP, direct measurements of BR seldom performed, probably due to the relatively long incubation times required and low sensitivity. In this study, we report direct measurements of BR in the southern ECS. However, because of the limited number of 12 BR data points, the relationship between BR and environmental and ecological parameters was evaluated to obtain BR_{est} throughout the study area. BR_{est} can be estimated from temperature, DOC, community respiration, and bacterial abundance and production (Robinson, 2008). Robinson (2008) suggested that BP was the most common parameter for the estimation of BR_{est}. Our data also presented the most significant relationship between BR and BP as $BR_{est} = 6.21*BP^{0.56}$ ($r^2 = 0.66$; $p < 0.01$; $n = 12$). Therefore, BP was used to estimate BR_{est} at all depths at all stations. The depth-integrated BR (IBR) ranged from 709–2822 mgC m^{-2} d^{-1}, also showing the highest IBR at station 9 (**Table 1**). Bacterial production and respiration allow the calculation of BGE, which is defined as the proportion of the bacterial carbon demand that is used for bacterial production. The depth-integrated BGE ranged from 0.04–0.08 with an average of 0.06 ± 0.01. The BGE in this study was located at the lower end of the globally reported data: del Giorgio and Cole (2000) estimated BGE values in the open ocean and coastal areas to be 0.15 ± 0.12 (median 0.09) and 0.27 ± 0.18 (median 0.25), respectively; Robinson (2008) summarized slightly lower BGE values of 0.14 ± 0.14 (median 0.08) and 0.19 ± 0.16 (median 0.16) for open ocean and coastal waters, respectively. The BGE at upwelling station 9 (0.08) was higher than that at the other stations, which was comparable to the BGE of 0.08 in the coastal upwelling of the NE Atlantic (González et al., 2003).

Phytoplankton-Bacteria Coupling

The coupling between phytoplankton and heterotrophic bacteria has been investigated for decades (e.g., Cole et al., 1988). The strength of coupling has been widely evaluated through the relationship between particulate primary and bacterial production (Cole et al., 1988). However, the coupling between phytoplankton and bacteria is mainly linked via labile phytoplankton-released DOC. Therefore, the strength of coupling was further defined as how much DPP meets BCD (Morán et al., 2002; Fouilland and Mostajir, 2010). Morán et al. (2002) calculated the DPP:BCD and suggested a strong coupling (104%) at offshore stations and a weak coupling (7%) at shelf stations. Moreover, Fouilland and Mostajir (2010) defined a weak coupling when DPP fulfilled less than 10% of BCD. In this study, the depth-integrated DPP to BCD ratio ranged from 5.5–77.1%. Weak coupling of 5.5 and 8.7% occurred at stations 3 and 5, respectively; where the dominant water mass is the oligotrophic Taiwan Strait waters. On the other hand, stronger coupling of 53.8 and 77.1% occurred at the upwelling stations 9 and 11, respectively. These results indicat that nutrient inputs from the upwelling enhanced primary production and subsequent coupling between phytoplankton and bacteria.

Overall, depth-integrated TPP did not meet the BCD in the southern ECS except at station 11 (**Table 1**), i.e., the system was heterotrophic (Production/Respiration <1). At the strongest upwelling station 11, depth-integrated TPP exceeded BCD at a TPP:BCD of 154%. There were three major uncertainties during the incubation and calculation. First, the ^{14}C-based primary production measurements included algal respiration and bacterial consumption of newly produced DPP and led to underestimated values. The loss of algal respiration and bacterial uptake of DPP during experiments vary widely, with averages

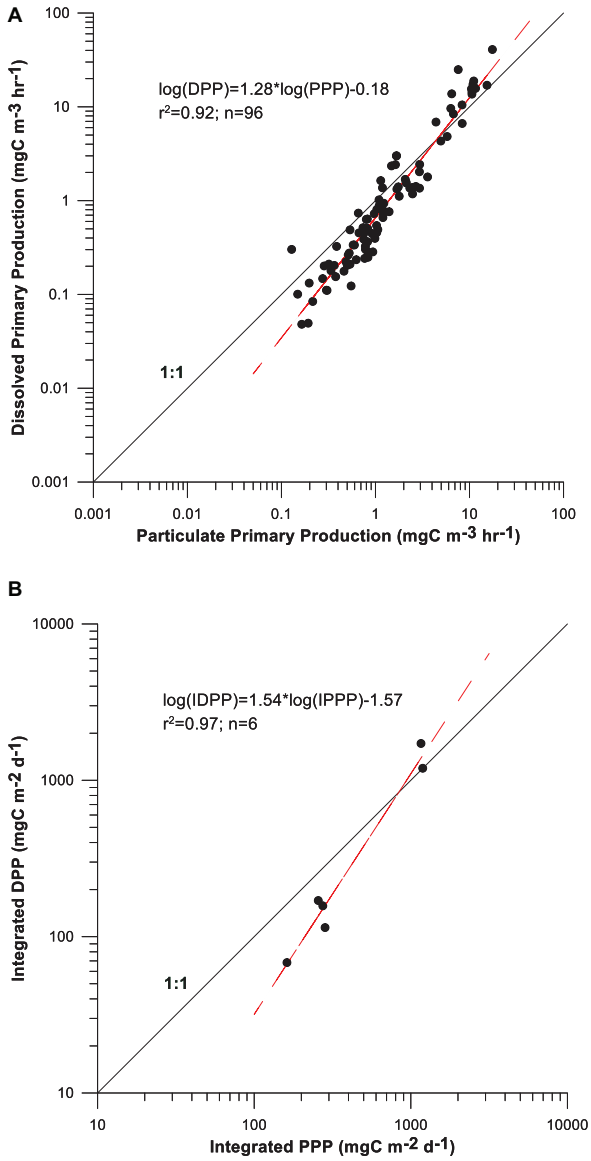

FIGURE 3 | Log-log relationship between particulate (PPP) and dissolved primary production (DPP) with all pooled **(A)** volumetric; **(B)** depth-integrated measurements. In both **(A)** and **(B)**, the slope of the simple linear regression was significantly greater than 1 (*t*-test, $p < 0.01$).

of approximately 36% (Duarte and Cebrián, 1996) and 46% (Baines and Pace, 1991), respectively. Secondly, the standard pre-filtration procedure of BR determination and incubation at surface water temperatures rather than is situ sampled depth temperatures might introduce an overestimation of at least 15% in the subsurface BR values (see more detail in **Appendix 2**). The third uncertainty was from the use of conversion factors. The bacterial RQ, defined as the production of CO_2 from the consumption of O_2 during respiration ($RQ = \Delta CO_2/-\Delta O_2$), directly affected the BR estimates. Although most reported RQ ratios are between 0.6 and 0.9, a recent compilation showed ratios ranging from <0.3 to >3.1 (Robinson, 2019). RQ ratios are associated with the composition of the dissolved organic matter (DOM) substrate: lower ratios are associated with labile DOM and higher ratios are associated with refractory DOM. Bacterial consumption of phytoplankton-released DOM, which is generally considered easy-to-use DOM, may lead to lower RQ ratios. In addition, the use of conversion factors of 2×10^{18} cells mol^{-1} thymidine and 20 fg $cell^{-1}$ for thymidine method could lead to overestimation of BP values (Ducklow, 2000).

Considering the uncertainties of algal respiration, bacterial consumption of DPP, BR overestimation, and conversion factors would lead upwelling stations to be strongly coupled or autotrophic (i.e., TPP exceeds BCD), whereas other stations remained heterotrophic. Then, the next question is what organic carbon sources fulfill the BCD? Decoupling or uncoupling between phytoplankton and bacteria has been reported in marine systems partly due to inorganic nutrient limitations (Carlson et al., 1994; Thingstad et al., 1997) or microbial responses on different time scales (Viviani and Church, 2017). Aside from temporary uncoupling, the organic carbon supplies other than DPP could be from sloppy feeding by protozoans (Nagata and Kirchman, 1992) or metazoans (Jumars et al., 1989) and viral lysis (Gobler et al., 1997). However, the ultimate origin of these organic sources is also photosynthetic carbon and should not be excluded from the TPP. Bacterial uptake of semi-labile or refractory DOC has been reported in oligotrophic oceans (Cherrier et al., 1999). With a low turnover rate, the uptake of old carbon should be a minor process to sustain BCD. Photolysis has been recognized to transform refractory DOC to the labile form (Moran and Zepp, 1997), but the role of photochemical reactions in bacterial growth remains unclear. The fact that BCD exceeds TPP in large areas of the ocean has long been recognized and discussed (del Giorgio et al., 1997; Duarte and Agustí, 1998; Duarte et al., 1999). In a global budget, del Giorgio and Duarte (2002) estimated significant allochthonous organic carbon sources, including riverine, atmospheric, and ancient inputs. However, whether the marine system is net heterotrophic or autotrophic remains an unsolved question.

DPP-PPP Relationship

The relationship between DPP and PPP has received interest because it provides information on how much photosynthetically fixed carbon is available for heterotrophic bacteria. In general, DPP and PPP are positively correlated. However, the slope of the log–log regression of DPP on PPP varies over a wide range. Previous studies suggested a slope between 0.6 and 0.8 (e.g., Anderson and Zeutschel, 1970; Berman and Holm-Hansen, 1974; Mague et al., 1980; Marañón et al., 2005). Morán et al. (2002) summarized a cross-marine-system data set including the Antarctic, Mediterranean and Atlantic Oceans and suggested an average slope of 0.62. However, another summary of cross-system data suggested a slope close to 1 (Baines and Pace, 1991). A slope close to 1 indicates that the ratio of photosynthetic carbon flowing to the microbial loop or grazing food web remains constant when system productivity changes. For a scenario with a slope less than 1, a greater proportion of photosynthetic carbon will flow into the microbial loop when the system is moving toward lower productivity. It is predicted that the surface ocean will become

warmer and more stratified as the Earth warms (Sarmiento et al., 2004; Behrenfeld et al., 2006). An increasingly stratified surface ocean will decrease nutrient supply from the deep ocean, support less phytoplankton, and lead to a less productive ocean. Boyce et al. (2010) concluded that global phytoplankton biomass has decreased at approximately 1% year^{-1} in response to global warming since 1900. Based on the suggestion by Morán et al. (2002), it is believed that organic carbon transport through the microbial loop will become more important in the future when the ocean is less productive.

In this study, we found the log(DPP) and log(PPP) were positively correlated with a slope larger than 1 (1.28) using simple linear regression.

$$\mathrm{Log\,(DPP)} = -0.18 + (1.28 \pm 0.04) * \mathrm{log\,(PPP)} \quad (r^2 = 0.92;\ p < 0.01;\ n = 96)$$

A slope larger than 1 indicates that more photosynthetic carbon flowed through the microbial loop in the more productive area (e.g., upwelling in this study). On the other hand, less photosynthetic carbon partitioning in the dissolved form will occur in the future less productive ocean. As phytoplankton exhibits different physiological responses to light and will perform differently with depth, the depth-integrated data have also been evaluated. The slope of the log(IDPP)-log(IPPP) regression was 1.54, which was even larger than the slope of log(DPP)-log(PPP) (**Figure 3B**).

$$\mathrm{Log\,(IDPP)} = -1.57 + (1.54 \pm 0.13) * \mathrm{log\,(IPPP)} \quad (r^2 = 0.97;\ p < 0.01;\ n = 6)$$

The slopes of volumetric and areal regression were both significantly greater than 1 (t-test, $p < 0.01$). These indicate that if the southern ECS becomes less productive, the microbial loop will more severely suffer in terms of the organic carbon supply.

DATA AVAILABILITY STATEMENT

The datasets generated for this study are available on request to the corresponding author.

AUTHOR CONTRIBUTIONS

T-YC and G-CG designed and managed the project. T-YC wrote the manuscript. T-YC, C-CL, and F-KS analyzed the data. All authors reviewed and approved the final manuscript.

FUNDING

Funding was provided by the Ministry of Science and Technology of Taiwan (grants #106-2611-M-019-024- and #107-2611-M-019-010-) awarded to T-YC.

ACKNOWLEDGMENTS

We deeply thank the crew of the R/V Ocean Researcher II for shipboard operations and water sampling.

REFERENCES

Abdel-Moati, A. (1990). Adsorption of dissolved organic carbon (DOC) on glass fibre filters during particulate organic carbon (POC) determination. *Water Res.* 24, 763–764. doi: 10.1016/0043-1354(90)90033-3

Agustí, S., and Duarte, C. M. (2013). Phytoplankton lysis predicts dissolved organic carbon release in marine plankton communities. *Biogeosciences* 10, 1259–1264. doi: 10.5194/bg-10-1259-2013

Amon, R. M. W., Fitznar, H.-P., and Benner, R. (2001). Linkages among the bioreactivity, chemical composition, and diagenetic state of marine dissolved organic matter. *Limnol. Oceanogr.* 46, 287–297. doi: 10.4319/lo.2001.46.2.0287

Anderson, G. C., and Zeutschel, R. P. (1970). Release of dissolved organic matter by marine phytoplankton in coastal and offshore areas of the northeast Pacific Ocean. *Limnol. Oceanogr.* 15, 402–404.

Aranguren-Gassis, M., Teira, E., Serret, P., Martínez-García, S., and Fernádez, E. (2012). Potential overestimation of bacterial respiration rates in oligotrophic plankto communities. *Mar. Ecol. Prog. Ser.* 453, 1–10. doi: 10.3354/meps09707

Baines, S., and Pace, M. L. (1991). The production of dissolved organic matter by phytoplankton and its importance to bacteria: patterns across marine and fresh water systems. *Limnol. Oceanogr.* 36, 1078–1090. doi: 10.4319/lo.1991.36.6.1078

Behrenfeld, M. J., O'malley, R. T., Siegel, D. A., Mcclain, C. R., Sarmiento, J. L., Feldman, G. C., et al. (2006). Climate-driven trends in contemporary ocean productivity. *Nature* 444, 752–755. doi: 10.1038/nature05317

Berman, T., and Holm-Hansen, O. (1974). Release of photoassimilated carbon as dissolved organic matter by marine phytoplankton. *Mar. Biol.* 28, 305–310. doi: 10.1007/bf00388498

Boyce, D. G., Lewis, M. R., and Worm, B. (2010). Global phytoplankton decline over the past century. *Nature* 466, 591–596. doi: 10.1038/nature09268

Carlson, C. A., Ducklow, H. W., and Michaels, A. F. (1994). Annual flux of dissolved organic carbon from the euphotic zone in the northwestern Sargasso Sea. *Nature* 371, 405–408. doi: 10.1038/371405a0

Cherrier, J., Bauer, J. E., Druffel, E. R. M., Coffin, R. B., and Chanton, J. P. (1999). Radiocarbon in marine bacteria: evidence for the ages of assimilated carbon. *Limnol. Oceanogr.* 44, 730–736. doi: 10.4319/lo.1999.44.3.0730

Cole, J. J., Findlay, S., and Pace, M. L. (1988). Bacterial production in fresh and saltwater ecosystems: a cross-system overview. *Mar. Ecol. Prog. Ser.* 43, 1–10. doi: 10.3354/meps043001

Cole, J. J., Likens, G. E., and Strayer, D. L. (1982). Photosynthetically produced dissolved organic carbon: an important carbon source for planktonic bacteria. *Limnol. Oceanogr.* 27, 1080–1090. doi: 10.4319/lo.1982.27.6.1080

del Giorgio, P. A., and Cole, J. J. (1998). Bacterial growth efficiency in natural aquatic systems. *Annu. Rev. Ecol. Syst.* 29, 503–541. doi: 10.1146/annurev.ecolsys.29.1.503

del Giorgio, P. A., and Cole, J. J. (2000). "Bacterial energetics and growth efficiency," in *Microbial Ecology of the Oceans*, ed. D. L.Kirchman (New York, NY: Wiley-Liss, Inc), 289–325.

del Giorgio, P. A., Cole, J. J., and Cimbleris, A. (1997). Respiration rates in bacteria exceed phytoplankton production in unproductive aquatic systems. *Nature* 385, 148–151. doi: 10.1038/385148a0

del Giorgio, P. A., and Duarte, C. M. (2002). Respiration in the ocean. *Nature* 420, 379–384. doi: 10.1038/nature01165

Druffel, E. R. M., Williams, P. M., Bauer, J. E., and Ertel, J. R. (1992). Cycling of dissolved and particulate organic matter in the open ocean. *J. Geophys. Res.* 97, 15639–15659.

Duarte, C. M., and Agustí, S. (1998). The CO2 balance of unproductive aquatic ecosystems. *Science* 281, 234–236. doi: 10.1126/science.281.5374.234

Duarte, C. M., Agustí, S., Del Giorgio, P. A., and Cole, J. J. (1999). Regional carbon imbalances in the oceans. *Science* 284:1733.

Duarte, C. M., Agustí, S., Vaque, D., Agawin, N. S. R., Felipe, J., Casamayor, E. O., et al. (2005). Experimental test of bacteria-phytoplankton coupling in the Southern Ocean. *Limnol. Oceanogr.* 50, 1844–1854. doi: 10.4319/lo.2005.50.6.1844

Duarte, C. M., and Cebrián, J. (1996). The fate of marine autotrophic production. *Limnol. Oceanogr.* 41, 1758–1766. doi: 10.4319/lo.1996.41.8.1758

Ducklow, H. (2000). "Bacterial production and biomass in the oceans," in *Microbial Ecology of the Oceans*, ed. D. L.Kirchmann (New York, NY: Wiley), 85–120.

Dugdale, R. C., and Goering, J. J. (1967). Uptake of new and regenerated forms of nitrogen in primary productivity. *Limnol. Oceanogr.* 12, 196–206. doi: 10.4319/lo.1967.12.2.0196

Fouilland, E., and Mostajir, B. (2010). Revisited phytoplanktonic carbon dependency of heterotrophic bacteria in freshwaters, transitional, coastal and oceanic waters. *FEMS Microbiol. Ecol.* 73, 419–429. doi: 10.1111/j.1574-6941.2010.00896.x

Fuhrman, J. A., and Azam, F. (1982). Thymidine incorporation as a measure of heterotrophic bacterioplankton production in marine surface waters: evaluation and field results. *Mar. Biol.* 66, 109–120. doi: 10.1007/bf00397184

Gasol, J. M., and del Giorgio, P. A. (2000). Using flow cytometry for counting natural planktonic bacteria and understanding the structure of planktonic bacterial communities. *Sci. Mar.* 64, 197–224. doi: 10.3989/scimar.2000.64n2197

Gasol, J. M., and Morán, X. A. G. (1999). Effects of filtration on bacterial activity and picoplankton community structure as assessed by flow cytometry. *Aquat. Microb. Ecol.* 16, 251–264. doi: 10.3354/ame016251

Gobler, C. J., Hutchins, D. A., Fisher, N. S., Cosper, E. M., and Sañudo-Wilhelmy, S. A. (1997). Release and bioavailability of C, N, P, Se, and Fe following viral lysis of a marine chrysophyte. *Limnol. Oceanogr.* 42, 1492–1504. doi: 10.4319/lo.1997.42.7.1492

Gong, G.-C., Chen, Y.-L. L., and Liu, K.-K. (1996). Chemical hydrography and chlorophyll a distribution in the East China Sea in summer: implications in nutrient dynamics. *Cont. Shelf Res.* 16, 1561–1590. doi: 10.1016/0278-4343(96)00005-2

González, N., Anadón, R., and Viesca, L. (2003). Carbon flux through the microbial community in a temperate sea during summer: role of bacterial metabolism. . *Aquat. Microb. Ecol* 33, 117–126. doi: 10.3354/ame033117

Huang, Y., Chen, B., Huang, B., Zhou, H., and Yuan, Y. (2019a). Potential overestimation of community respiration in the western Pacific boundary ocean: what causes the putative net heterotrophy in oligotrophic system?*Limnol. Oceanogr.* 64, 2202–2219. doi: 10.1002/lno.11179

Huang, Y., Laws, E., Chen, B., and Huang, B. (2019b). Stimulation of heterotroophic and autotroophic metabolism in the mixing zone of the Kuroshio current and northern South China Sea: implications for export production. *J. Geophys. Res.* 124, 2645–2661. doi: 10.1029/2018jg004833

Jumars, P. A., Penry, D. L., Baross, J. A., Perry, M. J., and Frost, B. W. (1989). Closing the microbial loop: dissolved carbon pathway to heterotrophic bacteria from incomplete ingestion, digestion and absorption in animals. *Deep Sea Res.* 36, 483–495. doi: 10.1016/0198-0149(89)90001-0

Litchman, E., Klausmeier, C. A., and Bossard, P. (2004). Phytoplankton nutrient competition under dynamic light regimes. *Limnol. Oceanogr.* 49, 1457–1462. doi: 10.4319/lo.2004.49.4_part_2.1457

López-Sandoval, D. C., Fernádez, A., and Marañón, E. (2011). Dissolved and particulate primary production along a longitudinal gradient in the Mediterranean Sea. *Biogeosciences* 8, 815–825. doi: 10.5194/bg-8-815-2011

Mague, T. H., Friberg, E., Hughes, D. J., and Morris, I. (1980). Extracellular release of carbon by marine phytoplankton; a physiological approach. *Limnol. Oceanogr.* 25, 262–279. doi: 10.4319/lo.1980.25.2.0262

Marañón, E., Cermeño, P., Fernádez, E., Rodríguez, J., and Zabala, L. (2004). Significance and mechanisms of photosynthetic production of dissoved organic carbon in a coastal eutrophic ecosystem. *Limnol. Oceanogr* 49, 1652–1666. doi: 10.4319/lo.2004.49.5.1652

Marañón, E., Cermeño, P., and Pérez, V. (2005). Continuity in the photosynthetic production of dissolved organic carbon from eutrophic to oligotrophic waters. *Mar. Ecol. Prog. Ser.* 299, 7–17. doi: 10.3354/meps299007

Martínez-García, S., Fernádez, E., Del Valle, D. A., Karl, D. M., and Teira, E. (2013). Experimental assessment of marine bacterial respiration. *Aquat. Microb. Ecol.* 70, 189–205. doi: 10.3354/ame01644

Massana, R., Pedró-Alió, C., Casamayor, E. O., and Gasol, J. M. (2001). Changes in marine bacterioplankton phylogenetic composition during incubations designed to measurebiogeochemically significant parameters. *Limnol. Oceanogr.* 46, 1181–1188. doi: 10.4319/lo.2001.46.5.1181

Moran, M. A., and Zepp, R. G. (1997). Role of photoreactions in the formation of biologically labile compounds from dissoved organic matter. *Limnol. Oceanogr.* 42, 1307–1316. doi: 10.4319/lo.1997.42.6.1307

Moran, S. B., Charette, M. A., Pike, S. M., and Wicklund, C. A. (1999). Differences in seawater particulate organic carbon concentration in samples collected using small- and large-volume methods: the importance of DOC adsorption to the filter blank. *Mar. Chem.* 67, 33–42. doi: 10.1016/s0304-4203(99)00047-x

Morán, X. A. G., and Alonso-Sáez, L. (2011). Independence of bacteria on phytoplankton? Insufficient support for Fouilland & Mostajir's (2010) suggested new concept. *FEMS Microbiol. Ecol.* 78, 203–205. doi: 10.1111/j.1574-6941.2011.01167.x

Morán, X. A. G., and Estrada, M. (2001). Short-term variability of photosynthetic parameters and particulate and dissolved primary production in the Alboran Sea (SW Mediterranean). *Mar. Ecol. Prog. Ser.* 212, 53–67. doi: 10.3354/meps212053

Morán, X. A. G., Estrada, M., Gasol, J. M., and Pedró-Alió, C. (2002). Dissolved primary production and the strength of phytoplankton-bacterioplankton coupling in contrasting marine regions. *Microbial. Ecol.* 44, 217–223. doi: 10.1007/s00248-002-1026-z

Nagata, T. (2000). "Production mechanisms of dissolved organic matter," in *Microbial Ecology of the Oceans*, ed. D. L.Kirchman (New York, NY: Wiley-Liss, Inc.), 121–152.

Nagata, T., and Kirchman, D. L. (1992). Release of macromolecular organic complexes by heterotrophic marine flagellates. *Mar. Ecol. Prog. Ser.* 83, 233–240. doi: 10.3354/meps083233

Norrman, B., Zweifel, U. L., Hopkinson, C. S.Jr., and Fry, B. (1995). Production and utilization of dissolved organic carbon during an experimental diatom bloom. *Limnol. Oceanogr.* 40, 898–907. doi: 10.4319/lo.1995.40.5.0898

Novak, M. G., Centiniæ, I., Chaves, J. E., and Mannino, A. (2019). The adsorption of dissolved organic carbon onto glass fiber filters and its effect on the measurement of particulate organic carbon: a laboratory and modeling exercise. *Limnol. Oceanogr. Meth.* 16, 356–366. doi: 10.1002/lom3.10248

Pai, S.-C., Gong, G.-C., and Liu, K.-K. (1993). Determination of dissolved oxygen in seawater by direct spectrophotometry of total iodine. *Mar. Chem.* 41, 343–351. doi: 10.1016/0304-4203(93)90266-q

Parsons, T. R., Maita, Y., and Lalli, C. M. (1984). *A Manual of Chemical and Biological Methods for Seawater Analysis*. New York, NY: Pergamon Press.

Platt, T., Gallegos, C. L., and Harrison, W. G. (1980). Photoinhibition of photosynthesis in natural assemblages of marine phytoplankton J. *Mar. Res.*38, 687–701.

Pomeroy, L. R., and Wiebe, W. J. (2001). Temperature and substrates as interactive limiting factors for marine heterotrophic bacteria. *Aquat. Microb. Ecol.* 23, 187–204. doi: 10.3354/ame023187

Robinson, C. (2008). "Heterotrophic bacterial respiration," in *Microbial Ecology of the Oceans*, ed. D. L.Kirchmann (Hoboken, NJ: Wiley-Blackwell), 289–325.

Robinson, C. (2019). Microbial respiration, the engine of ocean deoxygenation. *Front. Mar. Sci.* 5:533. doi: 10.3389/fmars.2018.00533

Sarmiento, J. L., Slater, R., Barber, R., Bopp, L., Doney, S. C., Hirst, A. C., et al. (2004). Response of ocean ecosystems to climate warming. *Global Biogeochem. Cycles* 18:GB3003.

Sherr, E. B., Sherr, B. F., and Sigmon, C. T. (1999). Activity of marine bacteria under incubated and in situ conditions. *Aquat. Microb. Ecol.* 20, 213–223. doi: 10.3354/ame020213

Shiah, F.-K., Liu, K.-K., Kao, S.-J., and Gong, G.-C. (2000). The coupling of bacterial production and hydrography in the southern East China Sea: spatial patterns in spring and fall. *Cont. Shelf Res.* 20, 459–477. doi: 10.1016/s0278-4343(99)00081-3

Thingstad, T. F., Hagstrom, A., and Rassoulzadegan, F. (1997). Accumulation of degradable DOC in surface waters: is it caused by a malfunctioning microbial loop?*Limnol. Oceanogr.*42, 398–404. doi: 10.4319/lo.1997.42.2.0398

Thomas, J. P. (1970). Release of dissolved organic matter from natural populations of marine phytoplankton. *Mar. Biol.* 11, 311–323. doi: 10.1007/bf00352449

Thornton, D. C. O. (2014). Dissolved organic mtter (DOM) release by phytoplankton in the contemporary and future ocean. *Eur. J. Phycol.* 49, 20–46. doi: 10.1080/09670262.2013.875596

Varela, M. M., Bode, A., Moran, X. A. G., and Valencia, J. (2006). Dissolved organic nitrogen release and bacterial activity in the upper layers of the Atlantic Ocean. *Microbial. Ecol.* 51, 487–500. doi: 10.1007/s00248-006-9054-8

Viviani, D. A., and Church, M. J. (2017). Decoupling between bacterial production and primary production over multiple time scales in the North Pacific Subtropical Gyre. *Deep-Sea Res. I* 121, 132–142. doi: 10.1016/j.dsr.2017.01.006

Webb, W. L., Newton, M., and Starr, D. (1974). Carbon dioxide exchange of Alnus rubra: a mathematical model. *Oecologia* 17, 281–291. doi: 10.1007/bf00345747

Weisse, T., and Scheffel-Möser, U. (1991). Uncoupling the microbial loop: growth and grazing loss rates of bacteria and heterotrophic nanoflagellates in the North Atlantic. *Mar. Ecol. Prog. Ser.* 71, 195–205. doi: 10.3354/meps071195

Wurl, O. (2009). *Practical Guidelines for the Analysis of Seawater*. Boca Raton, FL: CRC Press.

Wyatt, K. H., Tellez, E., Woodke, R. L., Bidner, R. J., and Davison, I. R. (2014). Effects of nutrient limitation on the release and use of dissolved organic carbon from benthic algae in Lake Michigan. *Freshwater Sci.* 33, 557–567. doi: 10.1086/675453

Conflict of Interest: The authors declare that the research was conducted in the absence of any commercial or financial relationships that could be construed as a potential conflict of interest.

APPENDIX 1

Calculations for Particulate and Dissolved Primary Production

P^B–E relationship of particulate and dissolved primary production was modeled by Eqs (1a) from Webb et al. (1974) or (1b) from Platt et al. (1980), representing the scenarios of without and with photoinhibition, respectively.

$$P^B(z) = P^B_m(z)\left(1 - e^{-\frac{\alpha(z)E}{P^B_m(z)}}\right) \tag{1a}$$

$$P^B(z) = P^B_s(z)\left(1 - e^{-\frac{\alpha(z)E}{P^B_s(z)}}\right)\left(1 - e^{-\frac{\beta(z)E}{P^B_s(z)}}\right) \tag{1b}$$

where P^B represents the chlorophyll-a normalized primary productivity in the unit of mgC (mgChl)$^{-1}$ h^{-1}; E represents the light intensity in the unit of μE m^{-2} s^{-1}; photosynthetic parameters P^B_m and α represent the maximum chlorophyll-a normalized primary productivity and the initial slope, respectively. P^B_m has the same unit as P^B while α has the unit of mgC (mgChl)$^{-1}$ h^{-1} (μE m^{-2} s^{-1})$^{-1}$. In Eq. 1b, P^B_s is the hypothetic maximum photosynthetic rate and has the same unit as P^B_m. The parameter β describes the intensity of photoinhibition and has the same unit as α. During photoinhibition, the real maximum photosynthetic rate would be given by,

$$P^B_m(z) = P^B_s(z)\left(\frac{\alpha(z)}{\alpha(z)+\beta(z)}\right)\left(\frac{\beta(z)}{\alpha(z)+\beta(z)}\right)^{\beta(z)/\alpha(z)} \tag{2}$$

The P^B–E parameters, together with surface PAR, attenuation coefficients, and Chl concentrations, were used to estimate the primary production at each depth.

$$PP(z) = \int_0^t Chl(z)P^B_m(z)(1 - e^{-\frac{\alpha(z)E(z,t)}{P^B_m(z)}})\mathrm{d}t \tag{3a}$$

$$PP(z) = \int_0^t Chl(z)P^B_s(z)(1 - e^{-\frac{\alpha(z)E(z,t)}{P^B_s(z)}})e^{-\frac{\beta(z)E(z,t)}{P^B_s(z)}}\,\mathrm{d}t \tag{3b}$$

$$E(z,t) = E_0(t)e^{-(K_d z)} \tag{4}$$

where $E_0(t)$ represents the incident surface PAR during the day, K_d represents the mean attenuation coefficient of PAR within the euphotic zone, and t represents the time from sunrise to sunset. The daily depth-integrated primary production can then be calculated within the euphotic depth (Z_e) as the following:

$$IPP = \int_0^{Z_e} PP(z)\,dz \tag{5}$$

APPENDIX 2

Potential Overestimate for Bacterial Respiration

The standard procedure for the determination of bacterial respiration (i.e., a direct measurement of oxygen consumption) may introduce errors and resulted in an overestimate of BR (e.g., Aranguren-Gassis et al., 2012; Martínez-García et al., 2013). One problem with the pre-filtration method is the inability to separate heterotrophic bacteria from autotrophic picophytoplankton (Robinson, 2019). Pre-filtration followed by a long incubation time period has long been recognized to lead to potential artifacts including the removal of bacterial competitors (i.e., large phytoplankton; Litchman et al., 2004) and predators (i.e., protozoa; Weisse and Scheffel-Möser, 1991; Robinson, 2008), the increase of substrate availability (Gasol and Morán, 1999; Sherr et al., 1999), and a change in bacterial community composition during incubation (Massana et al., 2001). These methodological limitations may cause anything from no effect to an overestimation of 11 folds in various environments, such as a higher percentage of the overestimation in oligotrophic areas compared to mesotrophic areas (Aranguren-Gassis et al., 2012), and a significant overestimation in the Atlantic Ocean but an insignificant effect in the Pacific Ocean (Martínez-García et al., 2013). Further investigation is needed in order to obtain a general quantification for these potential errors.

Moreover, in this study, incubations cooled with running surface water could introduce another overestimation for subsurface BR determinations since the incubations were performed 2–4°C higher than the *in situ* temperature (see **Figure 2A** in the main manuscript). The temperature effect on BR could be evaluated using Q_{10} values of 2–3 for aquatic bacteria (Pomeroy and Wiebe, 2001). Q_{10} represents the metabolic rate increase for a temperature increase of 10°C. Assuming the Q_{10} = 2, for instance, the temperature increase of 2–4°C above 20°C could lead to an overestimate of BR of 15–32% (**Figure A1**).

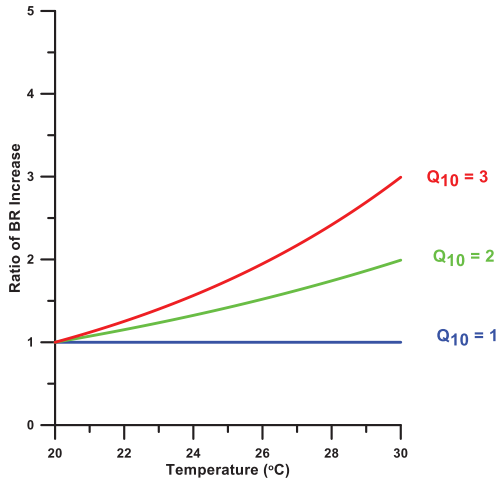

FIGURE A1 | Illustration of the temperature dependence of the rate of bacterial respiration (BR) at a range of Q_{10} values starting from 20°C.

APPENDIX 3

Comparison of Bacterial Respiration Models

Direct measurements of bacterial respiration (BR) were performed at two depths at each station in this study. Robinson (2008) found that bacterial production (BP) was the most significant parameter for the estimation of BR. Here we compared BR predictions from the following models and present the results in **Figure A2**:

$BR = 3.69\ BP^{0.58}$	Robinson, 2008
$BR = 7.09\ BP^{0.36}$	del Giorgio and Cole, 1998
$BR = 5.57\ BP^{0.41}$	del Giorgio and Cole, 2000
$BR = 6.21\ BP^{0.56}$	This study

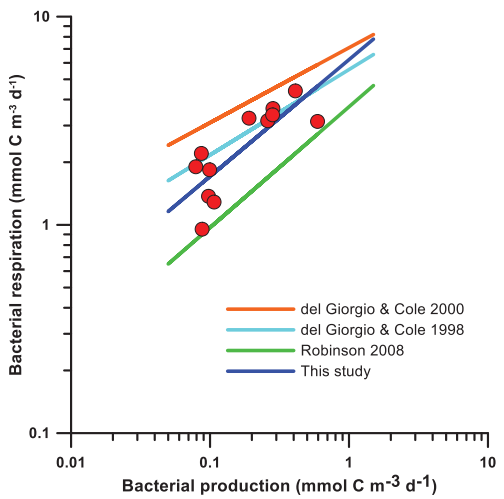

FIGURE A2 | Estimation of bacterial respiration from bacterial production using various models. Red dots denote the direct measurements of bacterial production and respiration.

del Giorgio and Cole's (2000) model tends to predict high BR values, while Robinson's (2008) model gives low BR values. del Giorgio and Cole (1998) and our models' predictions are similar and lie between the other two models.